atmosphere

MDPI

Supplementary material

Investigation of Summertime Ozone Formation and Sources of Volatile Organic Compounds in the Suburb Area of Hefei: A Case Study of 2020

Hui Yu [1,2], Qianqian Liu [2,3], Nana Wei [1,*], Mingfeng Hu [1], Xuezhe Xu [1], Shuo Wang [1], Jiacheng Zhou [1], Weixiong Zhao [1] and Weijun Zhang [1,3,*]

[1] Laboratory of Atmospheric Physico-Chemistry, Anhui Institute of Optics and Fine Mechanics, HFIPS, Chinese Academy of Sciences, Hefei 230031, China; huiyu@mail.ustc.edu.cn (H.Y.); mfhu@aiofm.ac.ca (M.H.); xzxu@aiofm.ac.cn (X.X.); wangs@aiofm.ac.cn (S.W.); zhoujch@aiofm.ac.cn (J.Z.); wxzhao@aiofm.ac.cn (W.Z.)

[2] Science Island Branch, Graduate School, University of Science and Technology of China, Hefei 230026, China; lqqwqs@mail.ustc.edu.cn

[3] School of Environmental Science and Optoelectronics Technology, University of Science and Technology of China, Hefei 230026, China

* Correspondence: weinn@aiofm.ac.cn (N.W.); wjzhang@aiofm.ac.cn (W.Z.)

Text S1. Analytical process for GC-MS/FID.

A 400 mL air sample from each canister was pumped into the preconcentrator (7200, Entech Instruments Inc., Simi Valley, CA, USA), equipped with three-stage cryotraps. In this process, water and carbon dioxide in the air sample were removed, and the sample was concentrated. Then the sample was injected into a gas chromatograph coupled with a mass selective detector and a flame ionization detector (TSQ 9000, Thermo Instruments Inc., Waltham, MA, USA). The C_2 ~ C_3 hydrocarbons were measured by the flame ionization detector (FID) channel with a TG BOND Q+ capillary column (30 m × 0.32 mm × 10 μm) (Thermo Instruments Inc., Waltham, MA, USA). The other VOC species were separated using the mass spectrometer detector (MSD) channel with a TG-624SilM capillary column (30 m × 0.53 mm × 3.0 μm) (Thermo Instruments Inc., Waltham, MA, USA). The gas chromatography temperature program was as follows: 40 °C (3 min); 40 °C to 90 °C at a rate of 3 °C min^{-1}; 90 °C to 130 °C at a rate of 15 °C min^{-1}; 130 °C to 200 °C at a rate of 5 °C min^{-1}; 200 °C (5 min).

The internal standard compounds (1.25 ppb) were acquired by diluting a standard gas (5 ppb) (Linde Electronics and Specialty Gases Inc., Danbury, CT, USA) comprising four species (bromochloromethane, 1,4-difluorobenzene, chlorobenzene-d5, and p-bromofluorobenzene). Five-point mixing ratio calibration curves ranging from 1 ppb to 7.5 ppb were established. The linear coefficients (R^2) of the standard curves for most of the species were above 0.99 (Table S1). The calibration curves were adjusted each day with a standard sample of 2 ppb, and the differences between the results and the corresponding values on the calibration curves should not exceed ± 30%. Otherwise, the curves were re-established.

Text S2. Detail procedure for positive matrix factorization (PMF).

The PMF model requires two input files, including a matrix of the concentrations (Conc) of VOC species and a matrix of concentration uncertainties (Unc). The uncertainty, Unc, is calculated by equations (1) and (2) as follows:

Citation: Yu, H.; Liu, Q.; Wei, N.; Hu, M.; Xu, X.; Wang, S.; Zhou, J.; Zhao, W.; Zhang, W. Investigation of Summertime Ozone Formation and Sources of Volatile Organic Compounds in the Suburb Area of Hefei: A Case Study of 2020. *Atmosphere* **2023**, *14*, 740. https://doi.org/10.3390/atmos14040740

Academic Editors: Lei Sun, Chen Wang and Leifeng Yang

Received: 23 March 2023
Revised: 13 April 2023
Accepted: 15 April 2023
Published: 19 April 2023

$$Unc = \sqrt{\left(EF \times x_{ij}\right)^2 + \left(0.5 \times MDL\right)^2} \quad (1)$$

$$Unc = \frac{5}{6} \times MDL \quad (2)$$

where *EF* represents the error fraction (%) of each species. x_{ij} is the species concentration (ppb), and *MDL* is the method detection limit (ppb). If the concentration exceeds the MDL, its uncertainty is calculated using equation (1). Suppose the concentration is less than or equal to the MDL. In that case, its uncertainty is calculated with equation (2), and the corresponding concentration is replaced by the value equal to half the MDL. Missing values were replaced by the median concentration of a species, with an uncertainty of four times the median [1,2].

Different factors were tested to obtain the optimal number of sources for the PMF solution. Each test executed 20 base runs to check the solution stability and the lowest Q value was selected as the base runtime solution. The Qtrue/Qexp values decreased gradually with an increasing number of factors. When the factor number increased to 7, the decrease in the amplitude became insignificant. Therefore, the factor number was determined as 7 after comparing the Qtrue/Qexp values.

The recommended ratio of Q(ture)/Q(robust) is less than 1.5. A ratio close to 1 is considered reliable [3,4]. In this study, the seven factors exhibited an acceptable Q(ture)/Q(robust) ratio of 1.00. The correlation coefficient (R^2) between the observed and predicted values of TVOCs for this solution was 0.95. High correlations were also found between the observed and predicted values of VOC species. The bootstrap method was used to evaluate the stability and rationality of the base run solution. The minimum correlation R^2 was set at 0.6, and 100 bootstrap runs were performed. All factors were mapped to more than 87% (Table S2), indicating that the base run solution was reasonable.

Text S3. The introduction of different VOC sources.

Factor 1 was identified as the combustion source, characterized by high proportions of low carbon alkanes, such as ethane (58.7%) and propane (43.1%), as well as halogenated hydrocarbons, such as chloromethane (31.9%) and chloroform (38%). Furthermore, the combustion process generates many short-chain and long-chain hydrocarbons, such as ethane and propane [5,6]. Chloromethane and chloroform are the markers of biomass combustion [7]. Thus, this source was identified as a combustion source.

Factor 2 was identified as the biogenic emission, characterized by high isoprene percentages. As the typical tracer for biogenic emission [8], isoprene showed good consistency with the diurnal profiles of temperature and solar radiation as shown in Figure S1. Hence, this source was identified as biogenic emission.

Factor 3 was identified as the fuel evaporation, characterized by high percentages of C_3 ~ C_5 alkanes with the contributions of *i*-butane, *n*-butane, *i*-pentane, and *n*-pentane of 29.2%, 27%, 44.5%, and 57.6%, respectively, which are the tracers of gasoline fuel evaporation [9]. Therefore, factor 3 was ascertained as fuel evaporation.

Factor 4 was rich in aromatic compounds, including ethylbenzene (47.9%), *m*/*p*-xylene (74.5%), and *o*-xylene (51.8%). The high abundances of these species strongly imply the solvent use source [10]. Here, factor 4 can be labeled as solvent utilization.

In factor 5, halogenated hydrocarbons have a dominant percentage. The contributions of dichloromethane, 1,2-dichloropropane, chloroform, and chlorobenzene were 51.5%, 59.5%, 33%, and 84%, respectively, with notable contributions of toluene (35.5%), ethylbenzene (36%), and *o*-xylene (38.1%). Dichloromethane, 1,2-dichloropropane, chloroform, and chlorobenzene are the important markers of industrial processes [11], while toluene, ethylbenzene, and *o*-xylene are emitted mainly by industrial production [12]. Therefore, factor 5 was identified as an industrial source.

Factor 6 was identified as vehicular emission, and was characterized by high proportions of alkenes, such as ethylene (52%), 1-butene (46.6%), and propylene (54.3%), which are the important indicators of vehicle exhaust [11]. In addition, propane (20.3%), *i*-pentane (20.3%), *n*-pentane (22.5%), 2-methylpentane (20.5%), and benzene (34.7%) also have relatively high proportions, of which C_3 ~ C_6 alkanes and benzene are the tracers of vehicle exhaust emissions. These species are considered typical products of incomplete combustion processes [10]. Thus, factor 6 was defined as a vehicular emission.

Factor 7 was enriched with halogenated hydrocarbons, mainly including methyl chloride (18%), dichloromethane (16.3%), and 1,2-dichloroethane (18%). These chemicals are typically emitted by industrial emissions [11], have a long lifetime in the atmosphere, and can be transported over long distances. This source also includes high concentrations of OVOCs, such as acetone (67.3%), 2-butanone (74.3%), and isopropanol (51%), which can be from the solvent usage and industrial production, as well as from the oxidation of VOCs [13]. As shown in Figure 4, the average X/E ratio during the observation period was 1.11, implying a high level of air mass aging and active photochemical reactions. The VOC source distribution in Zhengzhou had a similar characteristic [14]. As a result, factor 7 was defined as an aged air mass.

Table S1. The species information of VOCs measured at the AIOFM site.

VOC species	CAS number	Molecular formula	R^2 [1]
Alkanes			
Ethane	74-84-0	C_2H_6	0.9964
Propane	74-98-6	C_3H_8	0.9526
i-Butane	75-28-5	C_4H_{10}	0.9590
n-Butane	106-97-8	C_4H_{10}	0.9842
i-Pentane	78-78-4	C_5H_{12}	0.9996
n-Pentane	109-66-0	C_5H_{12}	0.9992
2,2-Dimethylbutane	75-83-2	C_6H_{14}	0.9989
2,3-Dimethylbutane	79-29-8	C_6H_{14}	0.9987
Cyclopentane	287-92-3	C_5H_{10}	0.9986
2-Methylpentane	107-83-5	C_6H_{14}	0.9992
3-Methylpentane	96-14-0	C_6H_{14}	0.9994
n-Hexane	110-54-3	C_6H_{14}	0.9991
2,4-Dimethylpentane	108-08-7	C_7H_{16}	0.9991
Methylcyclopentane	96-37-7	C_6H_{12}	0.9977
2-Methylhexane	591-76-4	C_7H_{16}	0.9992
Cyclohexane	110-82-7	C_6H_{12}	0.9974
2,3-Dimethylpentane	565-59-3	C_7H_{16}	0.9983
3-Methylhexane	589-34-4	C_7H_{16}	0.9990
2,2,4-Trimethylpentane	540-84-1	C_8H_{18}	0.9985
n-Heptane	142-82-5	C_7H_{16}	0.9981
Methylcyclohexane	108-87-2	C_7H_{14}	0.9991
2,3,4-Trimethylpentane	565-75-3	C_8H_{18}	0.9979
2-Methylheptane	592-27-8	C_8H_{18}	0.9989
3-Methylheptane	589-81-1	C_8H_{18}	0.9996

Octane	111-65-9	C_8H_{18}	0.9992
n-Nonane	111-84-2	C_9H_{20}	0.9992
n-Decane	124-18-5	$C_{10}H_{22}$	0.9992
Undecane	1120-21-4	$C_{11}H_{24}$	0.9996
Dodecane	112-40-3	$C_{12}H_{26}$	0.9998
Alkenes			
Ethene	74-85-1	C_2H_4	0.9185
Propene	115-07-1	C_3H_6	0.9939
1-Butene	106-98-9	C_4H_8	0.9818
1,3-Butadiene	106-99-0	C_4H_6	0.9953
trans-2-Butene	624-64-6	C_4H_8	0.9959
cis-2-Butene	590-18-1	C_4H_8	0.9989
1-Pentene	109-67-1	C_5H_{10}	0.9980
trans-2-Pentene	646-04-8	C_5H_{10}	0.9975
Isoprene	78-79-5	C_5H_8	0.9977
cis-2-Pentene	627-20-3	C_5H_{10}	0.9974
1-Hexene	592-41-6	C_6H_{12}	0.9987
Alkyne			
Acetylene	74-86-2	C_2H_2	0.9941
Halocarbons			
Freon12	75-71-8	CCl_2F_2	0.9330
Freon114	76-14-2	$C_2Cl_2F_4$	0.9223
Chloromethane	74-87-3	CH_3Cl	0.9567
Vinyl chloride	75-01-4	C_2H_3Cl	0.9700
Bromomethane	74-83-9	CH_3Br	0.9987
Chloroethane	75-00-3	C_2H_5Cl	0.9986
Freon11	75-69-4	$CFCl_3$	0.9996
1,1-Dichloroethylene	75-35-4	$C_2H_2Cl_2$	0.9982
Freon113	76-13-1	$C_2F_3Cl_3$	0.9996
Dichloromethane	75-09-2	CH_2Cl_2	0.9961
trans-1,2-Dichloroethene	156-60-5	$C_2H_2Cl_2$	0.9988
1,1-Dichloroethane	75-34-3	$C_2H_4Cl_2$	0.9991
cis-1,2-Dichloroethylene	156-59-2	$C_2H_2Cl_2$	0.9988
Chloroform	67-66-3	$CHCl_3$	0.9996
1,1,1-Trichloroethane	71-55-6	$C_2H_3Cl_3$	0.9989
Tetrachloromethane	56-23-5	CCl_4	0.9988
1,2-Dichloroethane	107-06-2	$C_2H_4Cl_2$	0.9993
1,2-Dichloropropane	78-87-5	$C_3H_6Cl_2$	0.9992
Bromodichloromethane	75-27-4	$CHBrCl_2$	0.9984
trans-1,3-Dichloropropene	10061-02-6	$C_3H_4Cl_2$	0.9993
cis-1,3-Dichloropropene	10061-01-5	$C_3H_4Cl_2$	0.9976

1,1,2-Trichloroethane	79-00-5	$C_2H_3Cl_3$	0.9990
Tetrachloroethylene	127-18-4	C_2Cl_4	0.9987
Dibromochloromethane	124-48-1	$CHBr_2Cl$	0.9979
1,2-Dibromoethane	106-93-4	$C_2H_4Br_2$	0.9983
Trichloroethylene	79-01-6	C_2HCl_3	0.9988
Chlorobenzene	108-90-7	C_6H_5Cl	0.9984
Bromoform	75-25-2	$CHBr_3$	0.9975
1,1,2,2-Tetrachloroethane	79-34-5	$C_2H_2Cl_4$	0.9991
1,3-Dichlorobenzene	541-73-1	$C_6H_4Cl_2$	0.9972
1,4-Dichlorobenzene	106-46-7	$C_6H_4Cl_2$	0.9971
Benzyl chloride	100-44-7	C_7H_7Cl	0.9961
1,2-Dichlorobenzene	95-50-1	$C_6H_4Cl_2$	0.9972
1,2,4-Trichlorobenzene	120-82-1	$C_6H_3Cl_3$	0.9982
Hexachloro-1,3-butadiene	87-68-3	C_4Cl_6	0.9940
OVOCs			
Acetaldehyde	75-07-0	C_2H_4O	0.9869
Acrolein	107-02-8	C_3H_4O	0.9964
Propanal	123-38-6	C_3H_6O	0.9987
Acetone	67-64-1	C_3H_6O	0.9977
Isopropanol	67-63-0	C_3H_8O	0.9991
MTBE	1634-04-4	$C_5H_{12}O$	0.9995
Methacrolein	78-85-3	C_4H_6O	0.9983
Vinyl acetate	108-05-4	$C_4H_6O_2$	0.9988
2-Butanone	78-93-3	C_4H_8O	0.9995
Butanal	123-72-8	C_4H_8O	0.9987
Ethyl acetate	141-78-6	$C_4H_8O_2$	0.9991
trans-2-Butenal	123-73-9	C_4H_6O	0.9945
Pentanal	110-62-3	$C_5H_{10}O$	0.9997
Methyl methacrylate	80-62-6	$C_5H_8O_2$	0.9990
4-Methyl-2-pentanone	108-10-1	$C_6H_{12}O$	0.9987
2-Hexanone	591-78-6	$C_6H_{12}O$	0.9979
Hexanal	66-25-1	$C_6H_{12}O$	0.9981
Benzaldehyde	100-52-7	C_7H_6O	0.9992
3-Methylbenzaldehyde	620-23-5	C_8H_8O	0.9933
Tetrahydrofuran	109-99-9	C_4H_8O	0.9994
1,4-Dioxane	123-91-1	$C_4H_8O_2$	0.9985
Aromatics			
Benzene	71-43-2	C_6H_6	0.9983
Toluene	108-88-3	C_7H_8	0.9984
Ethylbenzene	100-41-4	C_8H_{10}	0.9982
m/*p*-Xylene	106-42-3	C_8H_{10}	0.9991

o-Xylene	95-47-6	C_8H_{10}	0.9987
Styrene	100-42-5	C_8H_8	0.9992
Isopropyl benzene	98-82-8	C_9H_{12}	0.9991
n-Propyl benzene	103-65-1	C_9H_{12}	0.9996
4-Ethyltoluene	622-96-8	C_9H_{12}	0.9997
3-Ethyltoluene	620-14-4	C_9H_{12}	0.9997
1,3,5-Trimethylbenzene	108-67-8	C_9H_{12}	0.9985
2-Ethyltoluene	611-14-3	C_9H_{12}	0.9983
1,2,4-Trimethylbenzene	95-63-6	C_9H_{12}	0.9985
1,2,3-Trimethylbenzene	526-73-8	C_9H_{12}	0.9993
1,4-Diethylbenzene	105-05-5	$C_{10}H_{14}$	0.9984
1,3-Diethylbenzene	141-93-5	$C_{10}H_{14}$	0.9980
Naphthalene	91-20-3	$C_{10}H_8$	0.9998
Sulfide			
Carbon disulfide	75-15-0	CS_2	0.9969

[1] The correlation coefficients (R^2) of calibration curves for VOC species.

Table S2. The results of base bootstrap at the AIOFM site.

	Factor 1	**Factor 2**	**Factor 3**	**Factor 4**	**Factor 5**	**Factor 6**	**Factor 7**	**Unmapped**
Boot Factor 1	100	0	0	0	0	0	0	0
Boot Factor 2	0	100	0	0	0	0	0	0
Boot Factor 3	0	0	99	1	0	0	0	0
Boot Factor 4	0	0	0	100	0	0	0	0
Boot Factor 5	1	0	0	1	97	1	0	0
Boot Factor 6	1	0	4	2	4	87	2	0
Boot Factor 7	0	0	2	1	0	0	97	0

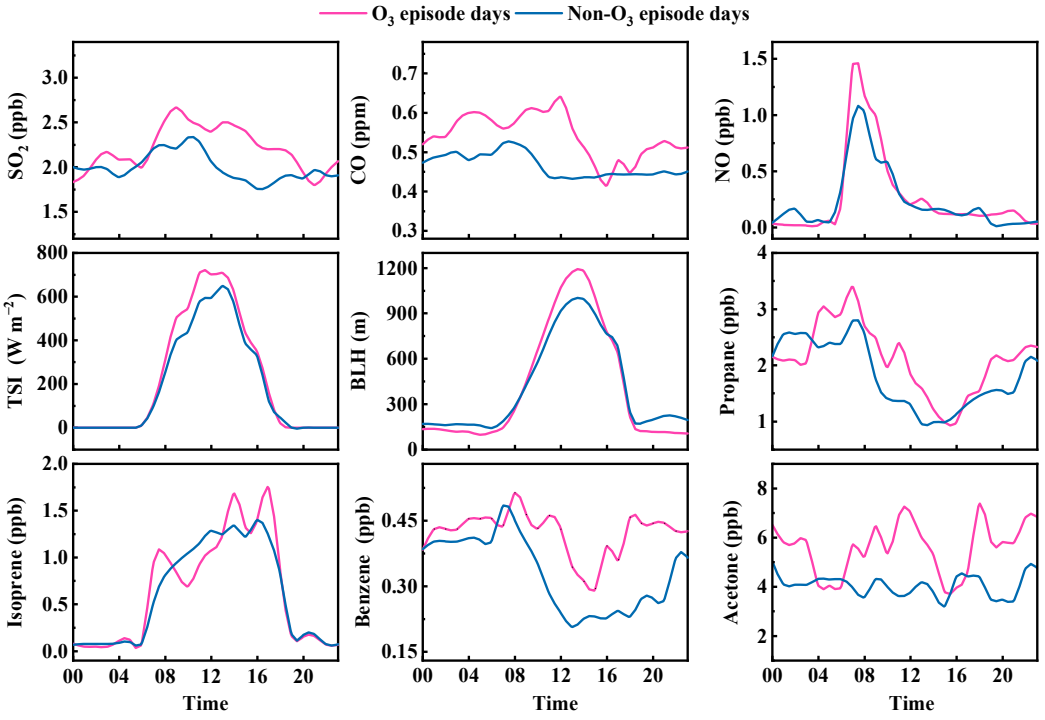

Figure S1. Diurnal variations of SO_2, CO, NO, total solar irradiance (TSI), boundary layer height (BLH), propane, isoprene, benzene, and acetone during the non-O_3 and O_3 episode days. The boundary layer height in Hefei was retrieved from the European Centre for Medium-Range Weather Forecasts model results (https://www.ecmwf.int/en/forecasts/datasets), accessed on 1 October 2020.

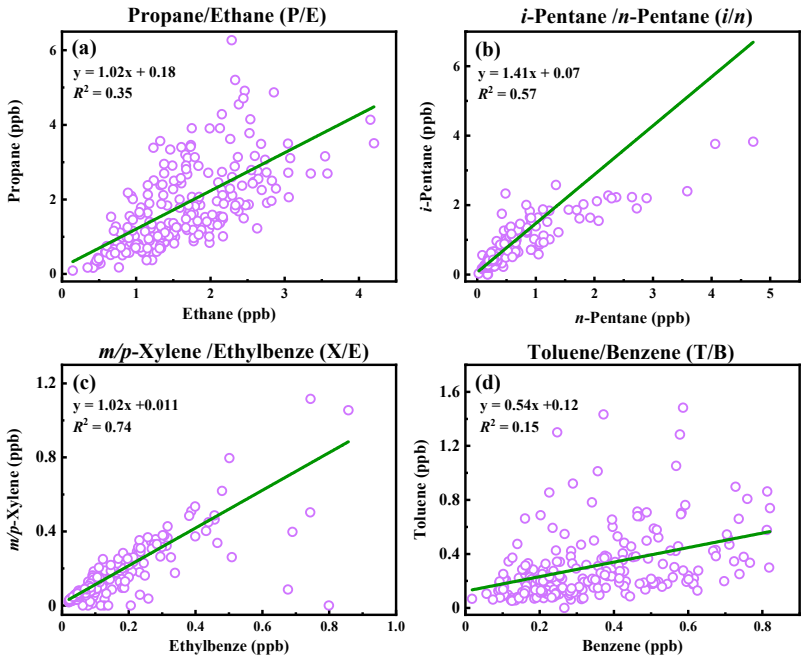

Figure S2. Linear correlations (R^2) between (a) propane/ethane, (b) *i*-pentane/*n*-pentane, (c) *m*/*p*-xylen/*o*-xylene, (d) toluene/benzene during the observation period.

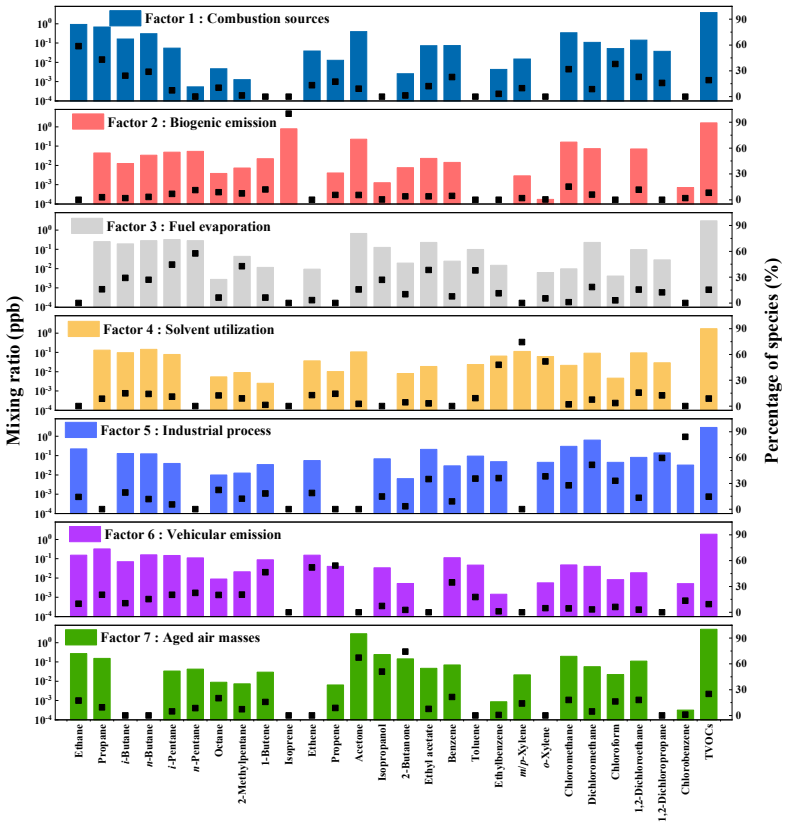

Figure S3. Source profiles and contribution percentages from each source during the observation period by the PMF model. The bar is a mixing ratio, and the dot is a percentage.

References

1. Norris, G.; Duvall, R. *EPA Positive Matrix Factorization (PMF) 5.0 Fundamentals and User Guide*; U.S. Environmental Protection Agency Office of Research and Development: Washington, DC, USA, 2014.
2. Shao, P.; An, J.; Xin, J.; Wu, F.; Wang, J.; Ji, D.; Wang, Y. Source apportionment of VOCs and the contribution to photochemical ozone formation during summer in the typical industrial area in the Yangtze River Delta, China. *Atmos. Res*. **2016**, *176*, 64–74. https://doi.org/10.1016/j.atmosres.2016.02.015.
3. Hui, L.; Liu, X.; Tan, Q.; Feng, M.; An, J.; Qu, Y.; Zhang, Y.; Cheng, N. VOC characteristics, sources and contributions to SOA formation during haze events in Wuhan, Central China. *Sci. Total Environ*. **2019**, *650*, 2624–2639. https://doi.org/10.1016/j.scitotenv.2018.10.029.
4. Song, M.; Li, X.; Yang, S.; Yu, X.; Zhou, S.; Yang, Y.; Chen, S.; Dong, H.; Liao, K.; Chen, Q.; et al. Spatiotemporal variation, sources, and secondary transformation potential of volatile organic compounds in Xi'an, China. *Atmos. Chem. Phys*. **2021**, *21*, 4939–4958. https://doi.org/10.5194/acp-21-4939-2021.
5. Liu, Y.; Shao, M.; Fu, L.; Lu, S.; Zeng, L.; Tang, D. Source profiles of volatile organic compounds (VOCs) measured in China: Part I. *Atmos. Environ*. **2008**, *42*, 6247–6260. https://doi.org/10.1016/j.atmosenv.2008.01.070.
6. Yan, Y.; Yang, C.; Peng, L.; Li, R.; Bai, H. Emission characteristics of volatile organic compounds from coal-, coal, gangue-, and biomass-fired power plants in China. *Atmos. Environ*. **2016**, *143*, 261–269. https://doi.org/10.1016/j.atmosenv.2016.08.052.
7. Xiong, C.; Wang, N.; Zhou, L.; Yang, F.; Qiu, Y.; Chen, J.; Han, L.; Li, J. Component characteristics and source apportionment of volatile organic compounds during summer and winter in downtown Chengdu, southwest China. *Atmos. Environ*. **2021**, *258*, 118485. https://doi.org/10.1016/j.atmosenv.2021.118485.
8. Shao, P.; An, J.; Xin, J.; Wu, F.; Wang, J.; Ji, D.; Wang, Y. Source apportionment of VOCs and the contribution to photochemical ozone formation during summer in the typical industrial area in the Yangtze River Delta, China. *Atmos. Res*. **2016**, *176*, 64–74. https://doi.org/10.1016/j.atmosres.2016.02.015.
9. Liu, Y.; Wang, H.; Jing, S.; Gao, Y.; Peng, Y.; Lou, S.; Cheng, T.; Tao, S.; Li, L.; Li, Y.; et al. Characteristics and sources of volatile organic compounds (VOCs) in Shanghai during summer: Implications of regional transport. *Atmos. Environ*. **2019**, *215*, 116902. https://doi.org/10.1016/j.atmosenv.2019.116902.

10. Chen, G.; Liu, T.; Ji, X.; Xu, K.; Hong, Y.; Xu, L.; Li, M.; Fan, X.; Chen, Y.; Yang, C.; et al. Source apportionment of VOCs and O_3 production sensitivity at coastal and inland sites of southeast China. *Aerosol Air Qual. Res*. **2022**, *22*, 220289. https://doi.org/10.4209/aaqr.220289.
11. Mo, Z.; Shao, M.; Lu, S. Compilation of a source profile database for hydrocarbon and OVOC emissions in China. *Atmos. Environ*. **2016**, *143*, 209–217. https://doi.org/10.1016/j.atmosenv.2016.08.025.
12. He, Z.; Wang, X.; Ling, Z.; Zhao, J.; Guo, H.; Shao, M.; Wang, Z. Contributions of different anthropogenic volatile organic compound sources to ozone formation at a receptor site in the Pearl River Delta region and its policy implications. *Atmos. Chem. Phys*. **2019**, *19*, 8801–8816. https://doi.org/10.5194/acp-19-8801-2019.
13. Sha, Q.; Zhu, M.; Huang, H.; Wang, Y.; Huang, Z.; Zhang, X.; Tang, M.; Lu, M.; Chen, C.; Shi, B.; et al. A newly integrated dataset of volatile organic compounds (VOCs) source profiles and implications for the future development of VOCs profiles in China. *Sci. Total Environ*. **2021**, *793*, 148348. https://doi.org/10.1016/j.scitotenv.2021.148348.
14. Li, Y.; Yin, S.; Yu, S.; Yuan, M.; Dong, Z.; Zhang, D.; Yang, L.; Zhang, R. Characteristics, source apportionment and health risks of ambient VOCs during high ozone period at an urban site in central plain, China. *Chemosphere* **2020**, *250*, 126283. https://doi.org/10.1016/j.chemosphere.2020.126283.